Development 124, 2633-2644 (1997)
Printed in Great Britain © The Company of Biologists Limited 1997
DEV1175

Development of branchiomotor neurons in zebrafish

Anand Chandrasekhar[1], Cecilia B. Moens[2], James T. Warren Jr.[1], Charles B. Kimmel[2] and John Y. Kuwada[1,*]

[1]Department of Biology, University of Michigan, Ann Arbor, MI 48109-1048, USA
[2]Institute of Neuroscience, University of Oregon, Eugene, OR 97403-1254, USA

*Author for correspondence (e-mail: kuwada@umich.edu)

SUMMARY

The mechanisms underlying neuronal specification and axonogenesis in the vertebrate hindbrain are poorly understood. To address these questions, we have employed anatomical methods and mutational analysis to characterize the branchiomotor neurons in the zebrafish embryo. The zebrafish branchiomotor system is similar to those in the chick and mouse, except for the location of the nVII and nIX branchiomotor neurons. Developmental analyses of genes expressed by branchiomotor neurons suggest that the different location of the nVII neurons in the zebrafish may result from cell migration.

To gain insight into the mechanisms underlying the organization and axonogenesis of these neurons, we examined the development of the branchiomotor pathways in neuronal mutants. The *valentino* ^{b337} mutation blocks the formation of rhombomeres 5 and 6, and severely affects the development of the nVII and nIX motor nuclei. The *cyclops* ^{b16} mutation deletes ventral midline cells in the neural tube, and leads to a severe disruption of most branchiomotor nuclei and axon pathways. These results demonstrate that rhombomere-specific cues and ventral midline cells play important roles in the development of the branchiomotor pathways.

Key words: zebrafish, hindbrain, branchiomotor neuron, axonogenesis, *valentino*, *cyclops*

INTRODUCTION

Intricate mechanisms have evolved in multicellular organisms for generating specific neuronal cell types and for interconnecting them to create functional circuits (Goodman and Shatz, 1993; McConnell, 1995). In vertebrates, the mechanisms underlying the specification and pathfinding of neurons that innervate craniofacial structures are relatively obscure, and are addressed in this report. The segmentally iterated pharyngeal arches, which give rise to the jaws and other branchial tissue, along with their supporting structures and musculature (Schilling and Kimmel, 1994), are innervated by branchiomotor neurons that differentiate in specific segments, or rhombomeres, within the hindbrain (Noden, 1983; Gilland and Baker, 1993). A 2:1 correspondence between the hindbrain rhombomeres and the pharyngeal arches is evident both at the level of neural crest migration, whereby neural crest arising in individual even-numbered rhombomeres contributes to a single arch (Noden, 1983; Lumsden et al., 1991; Akimenko et al., 1994), and at the level of motor innervation, whereby motor neurons differentiating in pairs of rhombomeres innervate a single arch. Thus, in the chick and mouse, the first pharyngeal (mandibular) arch is innervated by neurons in rhombomere 2 (r2) and r3, the second pharyngeal (hyoid) arch is innervated by neurons in r4 and r5, the third pharyngeal arch is innervated by neurons in r6 and r7, and the remaining pharyngeal arches are innervated by neurons in the caudalmost hindbrain (reviewed in Gilland and Baker, 1993).

The molecular basis of hindbrain segmentation and its influence on pharyngeal arch morphogenesis and innervation are being rapidly elucidated (Lumsden and Krumlauf, 1996). *Krox20*, *kreisler* and *Hoxa-1* are required for segmentation (Lufkin et al., 1991; Chisaka et al., 1992; Frohman et al., 1993; Schneider-Maunoury et al., 1993; Swiatek and Gridley, 1993; McKay et al., 1994), while expression of hox genes in rhombomere-specific patterns has been shown to be required for aspects of segment identity within the hindbrain (Lufkin et al., 1991; Chisaka et al., 1992; Goddard et al., 1996; Studer et al., 1996). Mutations in several of these genes affect the organization of the cranial nerves (Lufkin et al., 1991; Chisaka et al., 1992; Schneider-Maunoury et al., 1993; Swiatek and Gridley, 1993; McKay et al., 1994), and in some cases have been shown to affect the specification of particular branchiomotor nuclei (Lufkin et al., 1991; Schneider-Maunoury et al., 1993; Swiatek and Gridley, 1993; Goddard et al., 1996; Studer et al., 1996).

We wished to address the issue of branchiomotor neuron specification and pathfinding in the zebrafish embryo, a vertebrate that is particularly amenable to genetic analyses (Nusslein-Volhard, 1994; Driever et al., 1994; Kimmel, 1993; Kuwada, 1995). As a first step in this endeavor, we have characterized the positions and axon pathways of the zebrafish branchiomotor neurons. Our results demonstrate extensive similarities with the branchiomotor organization of other species, but also some unexpected differences, specifically with respect to the location of the nVII (facial) motor nucleus. We have also assessed the effect of mutations in *cyclops* (Hatta et al., 1991) and *valentino* (Moens et al., 1996) on branchiomotor neuron specification and pathfinding. *valentino*, the

zebrafish homolog of the mouse *kreisler* gene (Cordes and Barsh, 1994), is required for the development of rhombomeres 5 and 6 from their common precursor 'protosegment' (Moens et al., 1996; and unpublished observations). The branchiomotor defects observed in *valentino* and *cyclops* mutant embryos suggest that rhombomere-specific cues, rhombomere boundaries and hindbrain floor plate cells play important roles in the specification, organization and pathfinding of these motor neurons.

We have also addressed the issue of branchiomotor neuronal migration. While chick branchiomotor neurons do not appear to migrate longitudinally within the hindbrain, examination of branchiomotor nuclei in wild-type and *Hoxb-1*$^{-}$ mice suggests that facial motor neurons may migrate caudally during development (Fritzsch, 1996; Goddard et al., 1996; Studer et al., 1996). We studied the spatial regulation of two genes expressed by zebrafish branchiomotor neurons. Our observation that the distribution of presumptive branchiomotor neurons shifts caudally during development, taken together with our data on the branchiomotor phenotype of *valentino* mutant embryos, suggests that there may be extensive caudal migration of branchiomotor neurons in the zebrafish hindbrain after specification.

MATERIALS AND METHODS

Animals

Adult zebrafish were reared and maintained as described in Westerfield (1995). Embryos were collected from breeding colonies, staged and allowed to develop at 28.5°C to the required age. Throughout the text, the developmental age of the embryos will correspond to the number of hours elapsed since fertilization (hours post-fertilization, hpf) for embryos older than 24 hpf, and to the hpf based on somite number (Kimmel et al., 1995), for embryos younger than 24 hpf. To inhibit pigmentation, embryos were transferred to fish water containing 0.2 mM phenylthiourea (Sigma) between 18 and 22 hpf (Burrill and Easter, 1994). The *valentino* ^{b337} (Moens et al., 1996) and the *cyclops* ^{b16} (Hatta et al., 1991) mutations are ENU- and γ ray-induced mutations, respectively, and both appear to be null alleles (Moens et al., Halpern et al., unpublished observations).

Retrograde labeling of hindbrain neurons

Embryos were fixed overnight at 4°C in 4% paraformaldehyde in 100 mM PO_4 buffer (PB: 81 mM Na_2HPO_4, 19 mM $NaH_2PO_4.H_2O$, pH 7.4). The embryos were washed four times in PB and embedded in 0.7% agar (in PB) on a glass slide. The agar overlying the arches was removed to expose them and the embedded embryos were submerged in PB. The slide was mounted on a microscope stage and the appropriate arch was labeled with the fluorescent lipophilic dye, DiI (Molecular Probes, Eugene, OR), by pressure injection using a Picospritzer (General Valve, Fairfield, NJ). The injected embryos were incubated at 4°C in a dark humid chamber for 12-16 hours to allow the DiI to retrogradely label the arch-innervating neurons (Fig. 1E).

Photoconversion of DiI fluorescence

The fluorescent DiI signal of labeled neurons and axons was converted by photooxidation (Lubke, 1993) into a visible brown precipitate that was stable in subsequent procedures such as antibody staining, in situ hybridization and cryostat sectioning. Briefly, labeled embryos were released from the agar, deyolked and decapitated at the level of the third somite with microsurgical scissors. The head fragments were incubated in PB containing 0.5 mg/ml diaminobenzidine (DAB) for 15 minutes, and mounted dorsally in a drop of DAB/PB between coverslips using vaseline supports. The fluorescence in the labeled cells was used to photooxidize DAB into a brown reaction product. After photoconversion, the embryos were released from between the coverslips, washed once in PB, fixed overnight in 4% paraformaldehyde/PB; they then served as the starting material for other procedures.

The data presented in this paper on the developmental appearance and rhombomeric location of the branchiomotor neurons were obtained from retrograde-labeling experiments performed on embryos at 26-30 hpf (n=28), 30-36 hpf (n=142), 40 hpf (n=15) and 48-52 hpf (n=109).

Immunohistochemistry

Embryos were fixed in 4% paraformaldehyde/PB containing 1% dimethylsulfoxide (DMSO). Processing of embryos for immunohistochemistry with the acetylated α-tubulin antibody (Piperno and Fuller, 1985), the zn5 antibody (Trevarrow et al., 1990), the distal-less antibody (Panganiban et al., 1995) and the islet antibody (39.4D5, Korzh et al., 1993) was performed as described previously (Chitnis and Kuwada, 1990) with the following changes: the Triton X-100 concentration was increased to 0.2% and all the buffers contained 1% DMSO. All antibodies except anti-distal-less are monoclonal.

In situ hybridization

Digoxygenin-labeled RNA probes were synthesized with components from a kit using the manufacturer's instructions (Boehringer Mannheim). Hybridization of zebrafish embryos was performed as described in Westerfield (1995). Hybridization to sense RNA probes generated no detectable signal in embryos.

Cryostat sectioning

Fixed embryos were washed twice in PB and incubated overnight in 30% sucrose/PB. Embryos were embedded in Oct compound (Miles, Elkhart, IN), frozen and sectioned in a Reichert-Jung 2800 cryostat to obtain 14 μm sections. The sections were air dried and topped with coverslips under 70% glycerol.

RESULTS

Neurons innervating the mandibular arch are located in rhombomeres 2 and 3

Since the zebrafish offers several advantages for the study of neuronal development, we initiated a study of neurons innervating the pharyngeal arches of the zebrafish embryo. In order to determine the location of the arch-innervating neurons, their cell bodies were retrogradely labeled by injection of a fluorescent lipophilic dye, DiI, into the pharyngeal arches. The result of such an experiment, in which DiI was injected into the hyoid arch, is shown in Fig. 1E.

Efferent neurons were retrogradely labeled by DiI injection into the mandibular arch. After photoconversion of the DiI fluorescence in the labeled cells, the embryos were labeled with the zn5 antibody to identify hindbrain rhombomeres (Fig. 1A). The zn5 antibody labels many cell types including the axons of hindbrain commissural neurons that lie at rhombomere boundaries (Trevarrow et al., 1990). Rhombomeres were numbered on the basis of two criteria: (1) their locations relative to the otocyst, in particular r5, which is just medial to the otocyst at all the ages examined here (Kimmel et al., 1995; data not shown), and (2) the location of the zn5-labeled abducens motor nucleus in r5 (Kimmel et al., 1985; Trevarrow et al., 1990), which is conserved in vertebrates (Gilland and Baker, 1993). Furthermore, since the zn5-labeled commissural

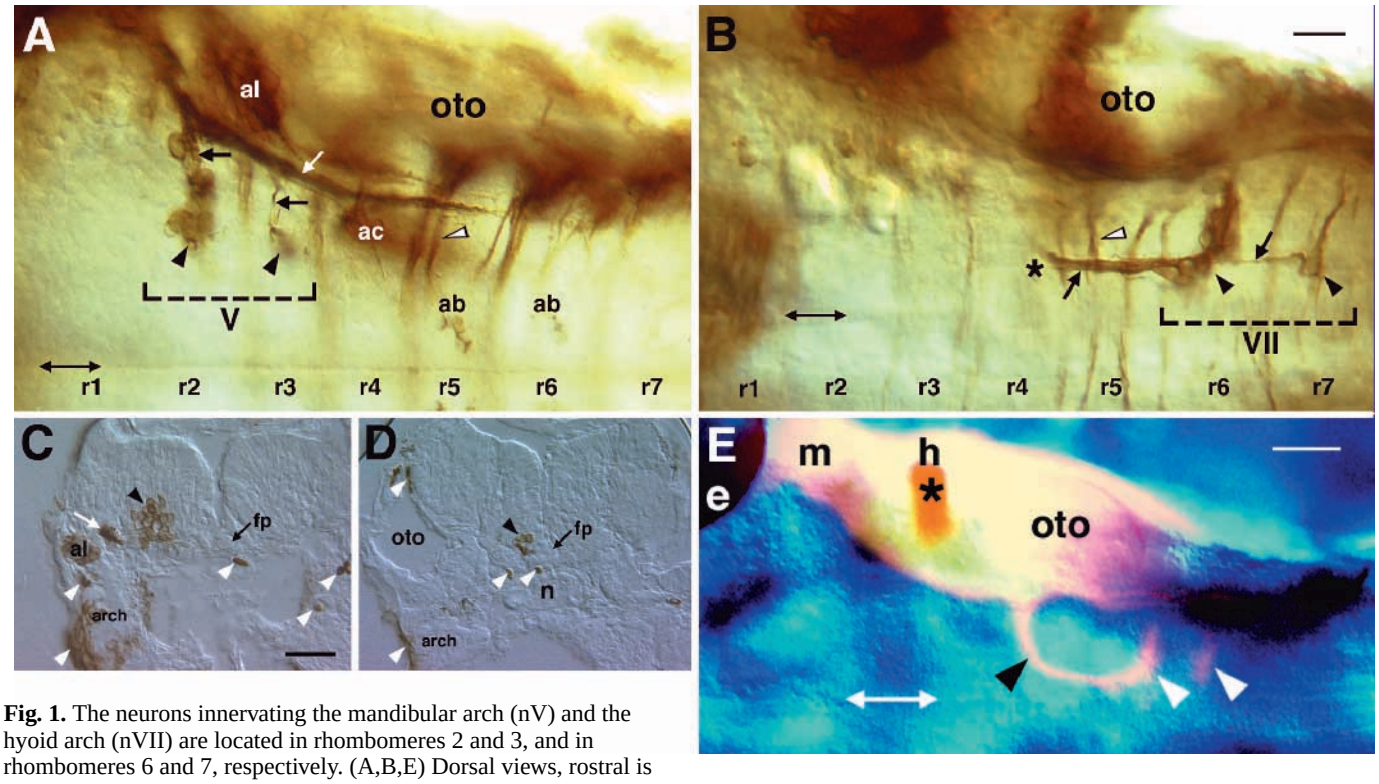

Fig. 1. The neurons innervating the mandibular arch (nV) and the hyoid arch (nVII) are located in rhombomeres 2 and 3, and in rhombomeres 6 and 7, respectively. (A,B,E) Dorsal views, rostral is to the left. (C,D) Transverse sections, dorsal is up. Double-headed arrows mark the midline. (A) nV and (B) nVII neurons were retrogradely labeled and visualized by photoconversion after DiI injection into the mandibular (A) and hyoid (B) arches on one side of 48 hpf (A) and 36 hpf (B) embryos. The embryos were subsequently processed for immunohistochemistry with the zn5 antibody, which labels hindbrain commissural axons that are located at rhombomere boundaries (white arrowheads). (A) The nV neurons (black arrowheads) lie in r2 and r3. Their axons (black arrows) join the trigeminal sensory axon bundle (white arrow), which was also labeled by DiI and photoconverted, before exiting the hindbrain in r2. The zn5 antibody also labels the anterior lateral line (al) and acoustic (ac) ganglia. (B) The nVII neurons (black arrowheads) lie in r6 and r7. Their axons (arrows) extend rostrally and parallel to the midline, within the hindbrain, before exiting in r4. The asterisk indicates the sharp lateral turn, the genu, of the motor axons. A portion of the efferent axons within r4 did not photoconvert. (C,D) Embryos with photoconverted nV (C) or nVII (D) neurons were cryostat-sectioned. (C) nV neurons (black arrowhead) in a section at the level of r2. The white arrow marks the trigeminal sensory axons (see A). (D) nVII neurons (black arrowhead) in a section at the level of r6. The white arrowheads in C and D indicate melanocytes or blood cells, both of which stain darkly during photoconversion even though they do not contain DiI fluorescence. (E) A composite Nomarski and fluorescence image showing the location of retrogradely labeled nVII neurons (white arrowheads) in the hindbrain after injection of the fluorescent, lipophilic dye DiI into the hyoid (h) arch. The axons (black arrowhead) exhibit a characteristic trajectory before exiting the hindbrain in r4. Although a fluorescence halo is visible over a large area, the DiI injection site (asterisk) was limited to the hyoid arch. ab, abducens motor nucleus; ac, acoustic ganglion; e, eye; fp, floor plate; h, hyoid arch; m, mandibular arch; n, notochord; oto, otocyst; r1-r7, rhombomeres 1-7. Bars, 20 μm (A,B); 40 μm (C,D); 40 μm (E).

axons exhibit distinctive trajectories in r5 (Fig. 1A), this pattern was used to identify r5 in younger embryos where the abducens nucleus was not labeled (e.g. Fig. 1B).

Two clusters of retrogradely labeled neurons, one each in r2 and r3, can be identified in 48 hpf embryos (Fig. 1A). The r2 cluster can be retrogradely labeled at 28 hpf, whereas the earliest time when the r3 cluster can be retrogradely labeled is between 36 and 40 hpf (data not shown). Consistent with this result, the axons extending into the mandibular arch are first seen as a few fibers at 27 hpf, medial to the trigeminal ganglion (data not shown), and extend into the rostral half of the arch between 30 and 36 hpf (Fig. 2A,B). At 48 hpf, the numbers of DiI-labeled cells in the r2 and r3 clusters are 14.8±5.6 and 10.9±5.4, respectively (n=17). The neurons are equidistant from the rhombomere borders, which were defined by the zn5 antibody-labeled hindbrain commissural axons (Trevarrow et al., 1990). A transverse section through r2 in a 48 hpf embryo (Fig. 1C) reveals that the motor neurons are also equidistant from the pial and ventricular surfaces of the hindbrain. The axons from each cluster fasciculate and extend laterally away from the midline until they encounter the afferent fibers of the trigeminal sensory neurons (Fig. 1A). The efferent axons join the trigeminal sensory axon bundle, turn rostrolaterally and exit the hindbrain in r2.

The growth cones of the mandibular arch-innervating neurons in the zebrafish have been shown to be closely associated with precursor cells that give rise to specific jaw muscles (Hatta et al., 1990). In addition, the relatively lateral position of these neurons (compare Fig. 1C and D), and the close association of their axons with the trigeminal afferent axons, are in accord with the anatomy of trigeminal motor neurons (nV) in other vertebrates (Moody and Heaton, 1983). Furthermore, the hindbrain exit points of the zebrafish axons extending into the mandibular and other arches (Fig. 2, and summarized in Fig. 4) are the same as those described for branchiomotor neurons in the chick (Lumsden and Keynes, 1989) and the mouse

(Marshall et al., 1992; Carpenter et al., 1993). Taken together, these observations indicate that the efferent neurons being studied are most likely to represent the zebrafish branchiomotor neurons, and will be referred to as such throughout the rest of the paper. However, these neuronal clusters may contain some non-branchiomotor efferent neurons.

Branchiomotor neurons innervating the hyoid arch (nVII) are located in rhombomeres 6 and 7

The nVII neurons were retrogradely labeled by DiI injection into the hyoid arch (Fig. 1E). Two clusters of nVII neurons, one each in r6 and r7, can be labeled in 36 hpf embryos (Fig. 1B). Although both motor neuron clusters can be retrogradely labeled by 30 hpf (data not shown, see Fig. 5A), the r6 cluster labels more reliably than the r7 cluster between 30 and 48 hpf. At 36 hpf, the numbers of DiI-labeled cells in the r6 and r7 clusters are 9.3±4.7 cells (n=24) and 3.1±1.6 (n=11), respectively. A transverse section through r6 in a 36 hpf embryo (Fig. 1D) reveals that the motor neurons are very ventral and medial, almost adjacent to the floor plate cells. The axons from the two clusters fasciculate and extend rostrally along a medial pathway that is parallel to the midline (Fig. 1B). Tubulin labeling of the medial longitudinal fascicle (MLF) in embryos with photoconverted nVII axons shows that they are closely apposed to the MLF (data not shown). Within r4, the motor axons make a sharp turn away from the midline (the genu) and follow the rostromedial margin of the otocyst into the arch (Fig. 1B,E; see also Fig. 5A). Examination of tubulin- and distal-less-labeled embryos shows that the axons innervating the hyoid arch exit the hindbrain at 28-29 hpf (data not shown) at the dorsorostral margin of the otocyst, and have extended into the arch mesenchyme by 36 hpf (Fig. 2A,B).

Since the nVII neurons are located primarily in r4 and r5 in other vertebrates (Gilland and Baker, 1993), we verified the unusual location of these motor neurons in the zebrafish by anterogradely labeling their axons by DiI application to their cell bodies in r6 in 36 hpf embryos and found that the axon terminals were located within the hyoid arch (n=6; data not shown).

Branchiomotor neurons innervating the gill arches (nIX, nX) are located in rhombomere 7 and the caudalmost hindbrain

The nIX neurons were retrogradely labeled by DiI injection into the first gill arch in 48 hpf embryos. These motor neurons are located very medially in a single cluster in r7 (Fig. 3A). The motor axons extend into r6 anteriorly along a medial pathway that is parallel to the midline, then make a sharp turn away from the midline (the genu) until they encounter the dorsocaudal margin of the

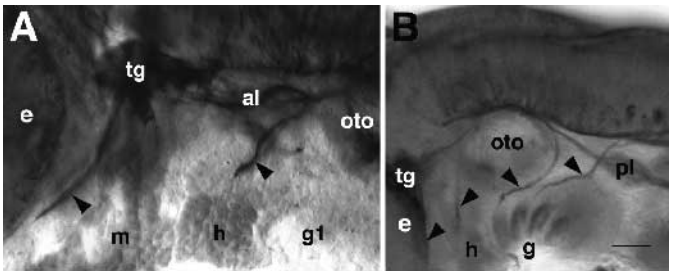

Fig. 2. Axons that innervate the pharyngeal arches exit the hindbrain from specific rhombomeres in a manner characteristic of branchiomotor axons. Both panels show lateral views; dorsal up, rostral to the left. (A) 30 hpf and (B) 36 hpf embryos were processed for immunohistochemistry with antibodies against acetylated α-tubulin, which labels various neurons (tg, al, pl) and axons (arrowheads), and the distal-less protein, which labels the pharyngeal arch mesenchyme (m, h, g1) in addition to other tissues. The axons innervating the pharyngeal arches exit from rhombomeres 2, 4, 6 and the caudalmost hindbrain, and probably correspond to the cranial nerves V, VII, IX and X, respectively (see text for details). al, anterior lateral line ganglion; e, eye; g1, first gill arch; g, all gill arches; h, hyoid arch; m, mandibular arch; oto, otocyst; pl, posterior lateral line ganglion; tg, trigeminal ganglion. Bar, 20 μm (A), 40 μm (B).

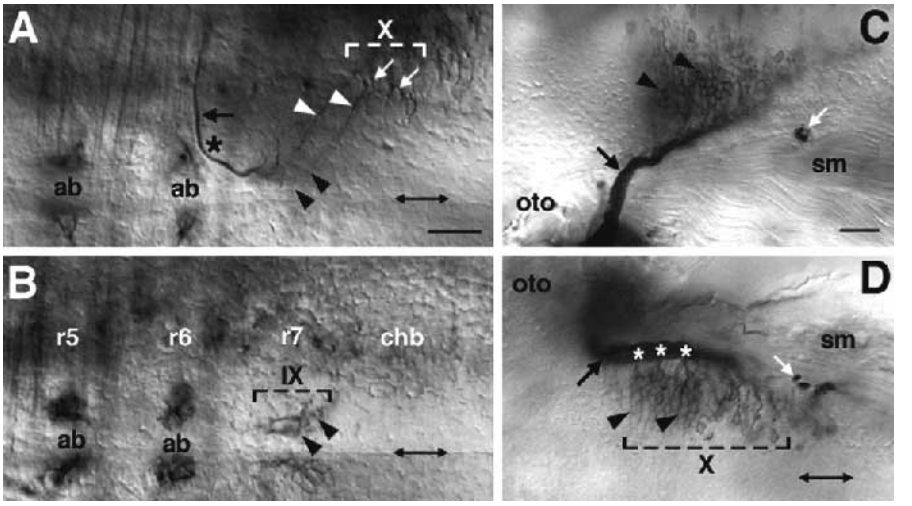

Fig. 3. The motor neurons innervating the first gill arch (nIX) and gill arches 2-5 (nX) are located in r7 and the caudalmost hindbrain, respectively. (A,B,D) Dorsal views. (C), lateral view. Rostral is to the left in all panels. Double-headed arrows mark the midline. (A,B) nIX neurons (black arrowheads) and their axons (black arrow) were retrogradely labeled and photoconverted after DiI injection into the first gill arch on one side in 48 hpf embryos. The embryos were subsequently processed for zn5 immunohistochemistry to label hindbrain commissural axons and the abducens nuclei. (A) The nIX axons exit the hindbrain in r6. The cell bodies, which are out of focus, lie in r7. Long lateral dendrites (white arrowheads) of nIX neurons contact inadvertently labeled nX neurons (white arrows). The asterisk indicates the sharp lateral turn, the genu, of the motor axons. (B) The nIX neurons express the antigen recognized by the zn5 antibody. The photoconverted nIX axons are out of focus, and could be seen only to the right of the midline, as in A. Two different embryos are depicted in A and B. (C,D) nX neurons (black arrowheads) and their axons (black arrow) were retrogradely labeled and photoconverted after DiI injection into the posterior gill arches on one side in 48 hpf embryos. (D) Axons from the nX neurons form three bundles that join a large axon fascicle (black arrow) at the sites indicated by the asterisks. The white arrows in C and D indicate stained blood cells, an artifact of photoconversion. ab, abducens motor nucleus; chb, caudalmost hindbrain; oto, otocyst; r5-7, rhombomeres 5-7; sm, somitic musculature. Bars, 20 μm (A,B); 20 μm (C,D).

otocyst and exit the hindbrain (Fig. 3A). The earliest axons exit the hindbrain at 30-32 hpf (data not shown), and extend along the ventrocaudal surface of the otocyst between 30 and 36 hpf (Fig. 2B). Interestingly, the nIX neurons are the only branchiomotor neurons that express the zn5-recognized antigen (Fig. 3B), which is encoded by the *DM-Grasp* gene (Kanki et al., 1994; Fashena, 1996).

The nX neurons were retrogradely labeled by DiI injection into gill arches 2-5 in 48 hpf embryos. The motor neurons are located in the caudalmost hindbrain (Fig. 3C,D). Although clustering of neurons is not evident, a dorsal view (Fig. 3D) suggests that these neurons extend axons ventrolaterally in several bundles, then turn anteriorly to form a large fascicle that exits from the caudalmost hindbrain (Figs 2B, 3C). At present, the correspondence between the axon bundles (Fig. 3D) and the gill arches that they innervate is not known.

The nIX neurons possess long lateral dendrites (Fig. 3A). In embryos where nIX and nX neurons were both inadvertently labeled (n=4), the nIX-associated dendrites contact the rostralmost nX neurons (Fig. 3A), suggesting that the motor neurons innervating the gill arches may interact.

Our observations on the zebrafish branchiomotor nuclei (summarised in Fig. 4) show that these motor nuclei share many characteristics of branchiomotor nuclei described in other vertebrates (Gilland and Baker, 1993). However, there is one major difference. The zebrafish nVII neurons are found in r6 and r7, and not in r4 and r5 as in the chick (all nVII neurons, Lumsden and Keynes, 1989) and the mouse (most nVII neurons, Marshall et al., 1992; Carpenter et al., 1993). Consequently, no zebrafish branchiomotor neurons are located in r4 and r5. Furthermore, the nIX and one cluster of nVII neurons are both located in r7, but their relative positions suggest that the two clusters are not mixed together (see Fig. 5B).

The zebrafish branchiomotor nuclei express the *isl1* and *tag1* genes

To study the appearance and organization of the branchiomotor neurons before their axons exit the hindbrain, we sought molecular markers that were expressed early by these neurons. We found that two neuronal genes, *isl1* (Inoue et al., 1994; Appel et al., 1995) and *tag1* (Warren et al., 1995), were expressed by branchiomotor neurons continuously between 30 and 48 hpf (Fig. 5; Warren et al., 1995).

The *isl1* gene, which encodes a LIM-homeodomain protein, is essential for motor neuron differentiation in the mouse (Pfaff et al., 1996). The islet 39.4D5 monoclonal antibody (Korzh et al., 1993) labels cells in the hindbrain that express *isl1* (Fig. 5; Inoue et al., 1994). Retrograde labeling of the various branchiomotor nuclei followed by islet immunolabeling shows that neurons in all of these nuclei (nV, nVII, nIX and nX) express *isl1* (Fig. 5A, data not shown). In addition to the branchiomotor nuclei, other islet-labeled cells in r5 and r6 may constitute the abducens motor nuclei (Fig. 5B).

The *tag1/axonin1* gene encodes an axonal cell surface glycoprotein that is transiently expressed on a number of sensory, motor and interneurons in the rat and chick (Furley et al., 1990; Stoeckli and Landmesser, 1995). The zebrafish homolog of *tag1* is similarly expressed by a subset of neurons, including clusters of hindbrain cells. Retrograde labeling of the branchiomotor neurons followed by in situ hybridization with a *tag1* riboprobe demonstrated that *tag1* is expressed by neurons in all of the branchiomotor nuclei, except nIX (Warren et al., 1995).

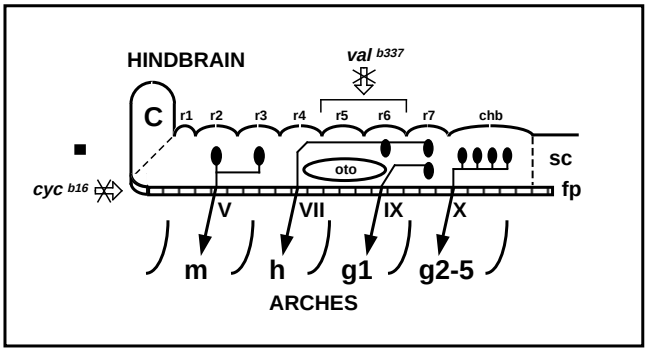

Fig. 4. Schematic figure of the hindbrain of a zebrafish embryo at 48 hpf depicting the cranial nerves (V, VII, IX and X), the locations of the branchiomotor nuclei, and the hindbrain phenotypes of the two mutations employed in this study. The rhombomeric swellings are exaggerated for clarity. The *valentino* ^{b337} mutation results in the failure of the precursor of r5 and r6 to subdivide and differentiate into the definitive rhombomeres (Moens et al., 1996). The *cyclops* ^{b16} mutation leads to the deletion of the floor plate cells (fp) at the ventral midline of the neural tube (Hatta et al., 1991). c, cerebellum; chb, caudalmost hindbrain; h, hyoid arch; g1-5, gill arches 1-5; m, mandibular arch; oto, otocyst; r1-7, rhombomeres 1-7; sc, spinal cord.

These results demonstrate that although neurons in all of the branchiomotor nuclei express *isl1*, the nIX nucleus differs from the other nuclei by expressing *DM-Grasp* (Fig. 3B), and not *tag1*. This heterogeneity in gene expression between nIX and nVII neurons reflects cellular differences that may enable their axons to innervate different arches in spite of their cell bodies being in the same environment (i.e. in r7).

The distribution of presumptive nVII neurons shifts caudally during development

Since no branchiomotor neurons are found in r4 and r5 in the zebrafish, we wondered whether the nVII motor neurons were born in r4 and r5, as in other vertebrates, and subsequently migrated into r6 and r7. To address whether nVII neurons may migrate across rhombomeres during development, we examined *isl1* and *tag1* gene expression in presumptive nVII neurons between 16 and 36 hpf. Assuming that cells express the *isl1* and *tag1* genes stably between 16 and 36 hpf, we predicted that if cells migrated from r4/5 into r6/7, then we would find *isl1*- and *tag1*-expressing cells in r4/5 early but not later. This was indeed what we found (Fig. 6).

At 16 hpf, a few *isl1*-expressing cells are located bilaterally in r4 (Fig. 6A), whereas there are no *tag1*-expressing cells. Rhombomere boundaries were estimated by designating the hindbrain spanning the central half of the otocyst as r5, and those spanning the rostral and caudal quarters of the otocyst as parts of r4 and r6, respectively. By 20 hpf, there are bilateral rostrocaudal columns of *isl1*- and *tag1*-expressing cells (Fig. 6C,D). The *isl1*-expressing cells span r4 through r7, while the *tag1*-expressing cells span r5 through r7. By 24 hpf, *isl1*-expressing cells are still found in r4 (Fig. 6E), while cells expressing high levels of *tag1* are found in r6 and r7 (Fig. 6F). By 36 hpf, most *isl1*- and *tag1*-expressing cells are confined to r6 and r7, where the nVII neurons are located (Fig. 6G,H). In

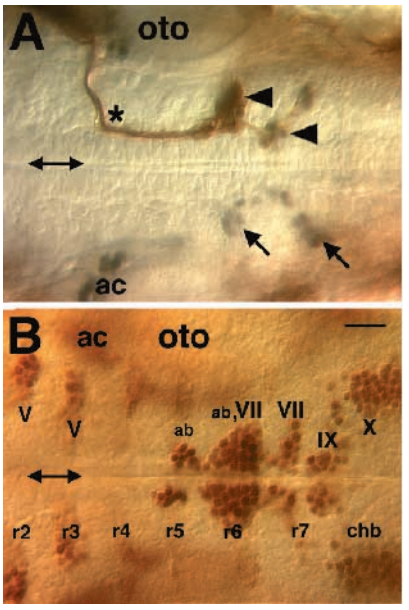

Fig. 5. Branchiomotor neurons express the *isl1* gene. Both panels show dorsal views with rostral to the left. Double-headed arrows mark the midline. (A) The nVII neurons were retrogradely labeled and photoconverted (brown signal) after DiI injection into the hyoid arch on one side in 30 hpf embryos. The embryos were subsequently processed for islet immunohistochemistry (black signal) to identify cells expressing the *isl1* gene. Arrowheads indicate photoconverted nVII neurons that also express *isl1*. Arrows indicate *isl1*-expressing nVII neurons on the opposite side. The asterisk indicates the sharp lateral turn, the genu, of the motor axons. (B) *Isl1*-expressing cells in the hindbrain of a 48 hpf embryo. The branchiomotor nuclei are labeled on the basis of results presented in A and from similar experiments performed to identify the other branchiomotor neurons (data not shown). V, nV neurons; VII, nVII neurons; IX, nIX neurons; X, nX neurons; ab, putative abducens neurons. ac, acoustic ganglion; chb, caudalmost hindbrain; oto, otocyst; r2-7, rhombomeres 2-7. Bar, 20 μm.

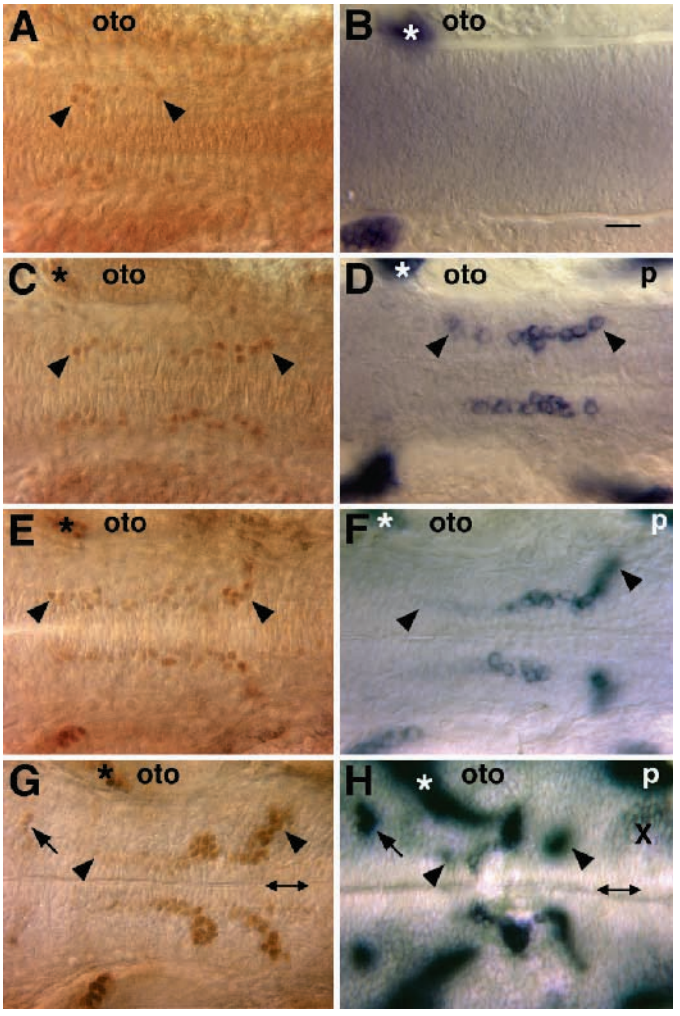

Fig. 6. The distribution of *isl1*- and *tag1*-expressing presumptive nVII neurons shifts caudally during development. All panels show dorsal views with rostral to the left. Double-headed arrows in (G) and (H) mark the midline. Embryos at various ages were processed for islet immunolabeling (A,C,E,G) or for in situ hybridization with a *tag1* riboprobe (B,D,F,H). (A,B) 16 hpf, (C,D) 20 hpf, (E,F) 24 hpf and (G,H) 36 hpf embryos. The black arrowheads in each panel indicate the positions of the most rostral and most caudal cells expressing the *isl1* or *tag1* genes, which are presumptive nVII neurons. Some of the *isl1*-expressing cells in r4/5 in G may be putative abducens neurons. The black arrows in G and H indicate nV neurons in r3. asterisk, acoustic ganglion; oto, otocyst; p, posterior lateral line ganglion. X, nX neurons. Bar, 20 μm.

contrast to the nVII neurons, presumptive nV neurons expressing *isl1* and *tag1* are located in r2 and r3 at 30 hpf (data not shown) and 36 hpf (Figs 6G,H and 7C), suggesting that they do not migrate after birth.

These results are consistent with the hypothesis that at least some nVII motor neurons are born in r4 and r5, and subsequently migrate into r6 and r7. However, we cannot rule out that the observed changes in the positions of *isl1*- and *tag1*-expressing cells in fact represent downregulation of these genes in cells in r4 and r5, and concomitant activation of these genes in different cells in r6 and r7.

Development of the nVII and nIX neurons is defective in *valentino* mutant embryos

Since the branchiomotor neurons occupy well-defined locations within specific rhombomeres, we wanted to know if rhombomere-specific cues played any role in the organization of these motor neurons and their axons. The *valentino* ^{b337} mutation is especially interesting because it blocks the formation of r5 and r6 from their precursor (rX), shortening the mutant hindbrain by one rhombomere (Fig. 4; Moens et al., 1996). Furthermore, the abducens motor nuclei normally located in r5 and r6 are missing in mutant embryos (Moens et al., 1996). Since some nVII neurons are located in r6, we predicted that the nVII nuclei would be affected in *val*$^{-}$ embryos. Indeed, we found that the nVII neurons, and surprisingly the nIX neurons, were severely affected in *val*$^{-}$ embryos.

Organization of the nV and nVII neurons were examined in 48 hpf embryos by DiI injection into the mandibular and hyoid arches, respectively. The nV neurons are found in two clusters in *val*$^{-}$ embryos, one each in r2 and r3, and appear indistinguishable from those in wild-type embryos (data not shown). The location and number of *tag1*-expressing cells in r2 and r3, the nV neurons, are also unaffected in *val*$^{-}$ embryos (Fig.

7C,D). In contrast, the nVII neurons and their axons were disrupted in *val*⁻ embryos. Two motor neuron clusters, in r6 and r7, are found in wild-type siblings (Fig. 7A). However, in all *val*⁻ embryos (*n*=30), the retrogradely labeled neurons are not clustered and are scattered over an approximately two rhombomere span, probably rX and r7 (Fig. 7B). The distribution of *tag1*-expressing cells also shows that the presumptive nVII neurons are disorganized in *val*⁻ embryos. In 36 hpf wild-type siblings, bilateral groups of *tag1*-expressing cells, one each in r6 and r7, are evident (Fig. 7C). However, in *val*⁻ embryos, the *tag1*-expressing cells are found in disorganized clumps spanning two rhombomeres (Fig. 7D). The distribution of *isl1*-expressing cells in 48 hpf wild-type and *val*⁻ embryos also demonstrates that the nVII neurons are disorganized in mutant embryos (Fig. 8D). Interestingly, the numbers of *tag1*-expressing presumptive nVII neurons (spanning r4 through r7) in 24 hpf wild-type and *val*⁻ embryos are similar at 18.7±3.6 (*n*=20) and 15.7±2.8 (*n*=14), respectively. These results demonstrate that the *valentino* ^{b337} mutation disrupts the organization of the nVII neurons, and suggest that the mutation does not affect their specification.

Although nVII axons do extend into the hyoid arch, some aspects of axonal pathfinding are affected in *val*⁻ embryos. In wild-type embryos, nVII axons are tightly fasciculated throughout their length in the hindbrain (Fig. 7A). In contrast, in *val*⁻ embryos, the nVII axons are significantly defasciculated, and join the main fascicle(s) at random points along its length (Fig. 7B). Interestingly, although the axons are frequently defasciculated, they always turn sharply away from the midline in r4 or in the rostral margin of rX, in a manner similar to wild-type axons. Since the retrograde labeling experiments provide information only on neurons that have correctly extended into the hyoid arch in mutant embryos, the number of neurons in rX/r7 that either do not extend axons or extend axons into inappropriate regions is not known.

The nIX neurons are also severely affected in *val*⁻ embryos. Immunolabeling of sagittal sections of 48 hpf wild-type and *val*⁻ hindbrains with the zn5 antibody shows that the zn5-labeled cell bodies in r7 corresponding to the nIX neurons (Figs 3B, 7E) are mostly missing in *val*⁻ embryos (Fig. 7F). Islet immunolabeling also shows that the *isl1*-expressing cells corresponding to the nIX nucleus are missing in 48 hpf *val*⁻ embryos (Fig. 8D). Consistent with these observations, the nIX axons that normally extend into the first gill arch (Figs 8A, 2B) are missing in *val*⁻ embryos (Fig. 8C). Interestingly, a novel branch of the cranial X nerve extends into the first gill arch in *val*⁻ embryos (Fig. 8C), which is reminiscent of an apparent fusion of the cranial IX and X nerves seen in *kreisler* mutant mouse embryos (McKay et al., 1994). The organization of the nX neurons in the caudalmost hindbrain, and the innervation of the posterior gill arches by nX axons are unaffected in *val*⁻ embryos (Fig. 8C, D). These results demonstrate that although the *val* ^{b337} mutation autonomously blocks the formation of only r5 and r6 (Moens et al., 1996), the mutation also disrupts the formation of the nIX neurons in r7.

Specification of branchiomotor neurons and pathfinding by their axons are defective in *cyclops* mutant embryos

Since floor plate-derived cues have been shown to be important

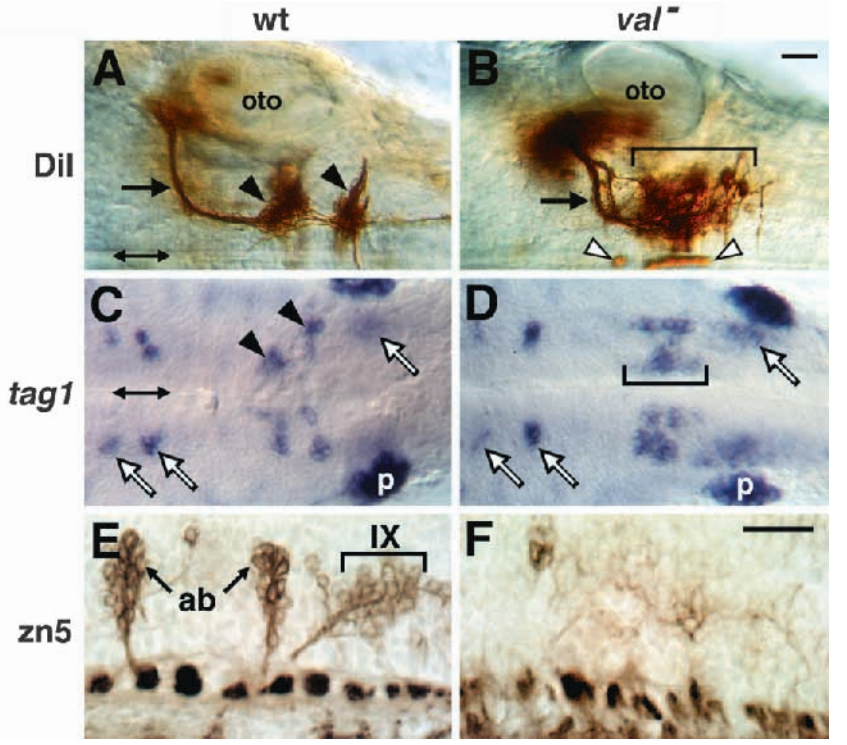

Fig. 7. The *val* ^{b337} mutation perturbs the development of the nVII and nIX neurons. (A-D), dorsal views. (E,F) Lateral views, dorsal up. Rostral is to the left in all panels. Double-headed arrows mark the midline. (A,B) nVII neuronal organization was determined by retrogradely labeling the motor neurons by DiI injection into the hyoid arch in 36 hpf wild-type sibling (A) and *val*⁻ (B) embryos. (A) The motor neurons are organized in two clusters (arrowheads) in r6 and r7. Their axons (arrow) exhibit the characteristics described earlier. (B) In the mutant embryo, there is a disorganized clump of motor neurons spanning two rhombomeres (bracket). Although the axons (arrow) possess wild-type-like trajectories, they are significantly defasciculated. White arrowheads indicate stained blood cells, an artifact of photoconversion. oto, otocyst. (C,D) Branchiomotor neurons were labeled by in situ hybridization to a *tag1* riboprobe in 36 hpf embryos. (C) In the wild-type embryo, *tag1*-expressing cells are found in bilateral groups (arrowheads), which correspond to the two nVII neuron clusters seen in A. (D) In the mutant embryo, the *tag1*-expressing cells are found in disorganized clumps spanning two rhombomeres (bracket). The white arrows indicate *tag1*-expressing nV neurons in r2 and r3, and nX neurons in the caudalmost hindbrain. Since the otocyst and other peripheral tissue were dissected away, the *tag1*-expressing cells of the acoustic ganglion are missing in C and D (compare to Fig. 6H). p, posterior lateral line ganglion. (E,F) nIX neurons were examined after zn5-immunolabeling of sagittal sections of 48 hpf embryos. (E) In the wild-type embryo, the nIX neurons and the abducens motor nuclei (ab) are readily identified (see also Fig. 3B). (F) In contrast, in the *val*⁻ embryo, both neuronal populations are mostly missing. The embryos depicted here were employed by Moens et al. (1996) to document the absence of the abducens neurons in *val*⁻ embryos. Bars, 20 μm (A-D) and (E,F).

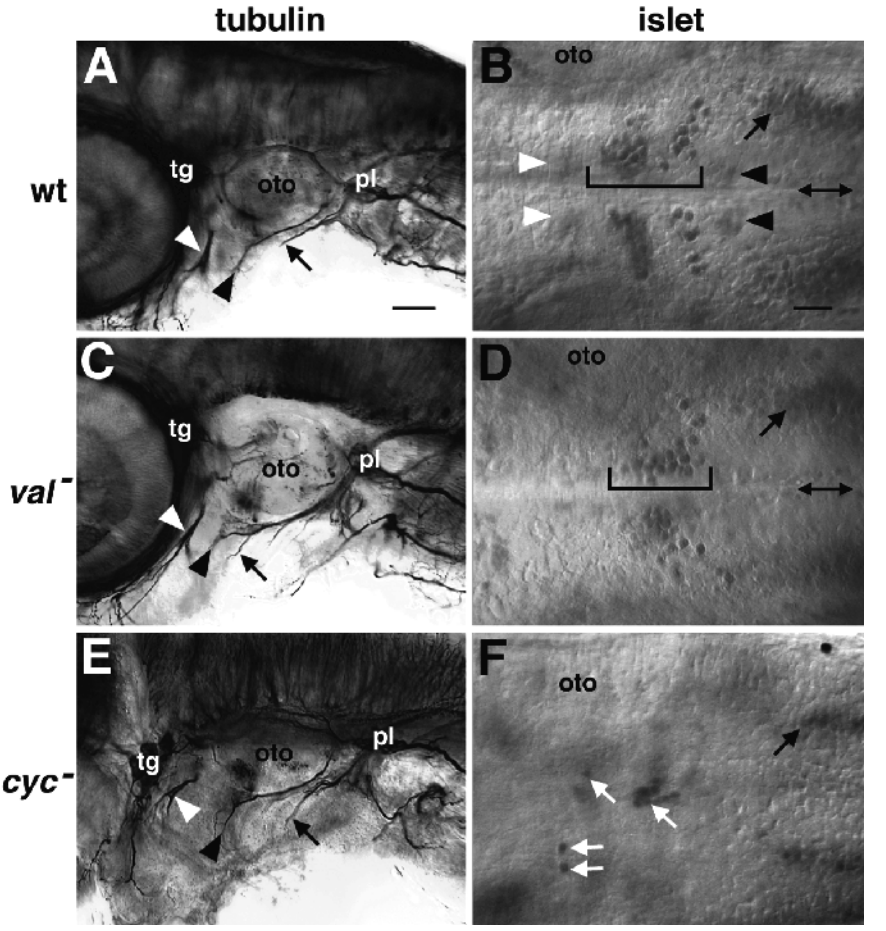

Fig. 8. Pharyngeal arch innervation (A,C,E) and *isl1* expression in the hindbrain (B,D,F) of 48 hpf *val*⁻ and *cyc*⁻ embryos. Arch innervation was visualized by tubulin immunolabeling, and *isl1* gene expression by islet immunolabeling. (A,C,E), lateral views. (B,D,F), dorsal views. Rostral is to the left in all of the panels. (A,C,E) White arrowhead indicates hyoid-arch innervating axons (nVII), black arrowhead indicates first gill arch-innervating axons (nIX, except C), and the arrow indicates second gill arch-innervating axons (nX). (A) The normal pattern of innervation in wild-type embryos was described earlier (Fig. 2B). (C) In the *val*⁻ embryo, nIX axons are missing. Instead, a novel branch of the posterior gill arch-innervating nX axons invades the first gill arch. (E) In the *cyc*⁻ embryo, all arches, except the mandibular, receive normal-looking axons. (B) *Isl1*-expressing cells in the wild-type hindbrain. The white arrowheads indicate out-of-focus cells that are putative abducens neurons (see Fig. 5B). The black arrowheads indicate out-of-focus nIX neurons. The two groups of nVII neurons are enclosed by the bracket. (D) In the *val*⁻ hindbrain, the nVII neurons are found in a disorganized clump. In addition, the nIX and the putative abducens neurons are missing (Fig. 7F; Moens et al., 1996). (F) In the *cyc*⁻ hindbrain, there are a few *isl1*-expressing cells (white arrows) whose neuronal identities cannot be ascertained. In B, D and F, oto indicates the location of the out-of-focus otocyst, and the black arrows indicate out-of-focus nX neurons. pl, posterior lateral line ganglion; tg, trigeminal ganglion. Bars, 40 μm (A,C,E); 20 μm (B,D,F).

for the specification of motor neurons (Tanabe and Jessell, 1996) and in neuronal pathfinding (Bernhardt et al., 1992a,b; Hatta, 1992; reviewed in Colamarino and Tessier-Lavigne, 1995) in the spinal cord, we examined the branchiomotor neurons and their axons in *cyclops* mutant embryos. The *cyclops* ^{b16} mutation leads to a deletion of the floor plate cells at the ventral midline of the neural tube at all rostrocaudal levels (Fig. 4; Hatta et al., 1991). We predicted that development of all of the branchiomotor nuclei would be affected in mutant embryos. Indeed, we found that the nV, nVII and nIX neurons were greatly reduced or absent in *cyc*⁻ embryos.

In 48 hpf *cyc*⁻ embryos, *isl1*- and *tag1*-expressing cells corresponding to the nV neurons are absent, and this is consistent with our failure to retrogradely label any neurons by DiI application to the mandibular arch (data not shown). Islet immunolabeling of 48 hpf *cyc*⁻ embryos shows that the numbers of nVII, nIX and abducens neurons are greatly reduced, while the nX neurons appear to be unaffected (Fig. 8F). We confirmed this observation for nVII neurons by our inability to retrogradely label these neurons, by DiI application to the hyoid arch, in about 60% (33/53) of 36 hpf mutant embryos (Table 1). Furthermore, when nVII neurons were successfully labeled, their numbers are greatly reduced when compared to wild-type siblings (Fig. 9B-D). A detailed analysis of branchiomotor neuron specification and the role of midline-derived cues in this process will be reported elsewhere (Chandrasekhar et al., unpublished observations).

Consistent with the greatly reduced number of nVII and nIX neurons in *cyc*⁻ embryos, tubulin immunolabeling revealed that the axons extending into the hyoid and first gill arches are absent in 36 hpf mutant embryos (data not shown). However, the pattern of axons extending into these arches in 48 hpf mutant embryos is similar to that in wild-type embryos (Fig. 8E). It is possible that a significant number of the arch-innervating axons at 48 hpf in fact represent afferent fibers of sensory neurons, whose cell bodies are not labeled by the tubulin antibody, and which are unaffected in 48 hpf *cyc*⁻ embryos. We confirmed this hypothesis for the cranial IX nerve by applying the lipophilic dye, DiI, at the nerve exit point in rhombomere 6 in 48 hpf embryos. We observed that comparable numbers of sensory neurons, lying between the otocyst and the first gill arch, were labeled in wild-type and *cyc*⁻ embryos, and that the trajectories of the afferent fibers of these neurons were identical to those of nIX motor axons in wild-type embryos (data not shown).

All of the branchiomotor axons project to ipsilateral targets in wild-type embryos. The nVII axons are especially interesting because they remain ipsilateral and extend rostrally in wild-type embryos, where they are in close proximity to the floor plate cells (Figs 1B, 5A). This observation suggests that floor plate-derived cues may play a role in nVII axon pathfinding, as demonstrated previously for other zebrafish neurons (Bernhardt et al., 1992a,b; Hatta, 1992). Consistent with this hypothesis, in about 50% (11/20) of *cyc*⁻ embryos with labeled

Table 1. nVII motor neuron specification and axonogenesis in *cyclops*⁻ embryos

Phenotype	Embryos injected	Embryos with no labeled cells	Embryos with labeled cells located			Comments
			Ipsilateral	Midline	Contralateral	
Wild type	29 (3)	2	27	0	0	Axons were tightly fasciculated in all embryos
cyc⁻	53 (4)	33	9	3	8	In 15 embryos with labeled cells, axons were defasciculated and strayed dramatically

All values are total number of embryos. Numbers in parentheses refer to the number of experiments performed.

nVII neurons, the cell bodies are located on the midline or on the contralateral side (Table 1, Fig. 9B,D), indicating that the axons readily cross the midline. Furthermore, in 75% (15/20) of the mutant embryos with labeled neurons, their axons are extremely defasciculated and neuronal processes frequently cross the midline regardless of the location of the cell bodies (Fig. 9B,C). These results suggest that floor plate-derived repulsive cues may play a role in the guidance of nVII motor axons.

DISCUSSION

Unusual location of the nVII neurons

The arrangement of the zebrafish branchiomotor nuclei and axon exit points is remarkably similar to those in the chick and the mouse (this report; Kimmel et al., 1985; Gilland and Baker, 1993). However, we found that the zebrafish nVII neurons are located in r6 and r7, whereas the nVII neurons are located exclusively in r4 and r5 in the chick (Lumsden and Keynes, 1989), and primarily in r4 and r5, with some in r6, in the mouse (Carpenter et al., 1993). Furthermore, the zebrafish nIX neurons are found only in r7, whereas nIX neurons in other vertebrates are found in r6 and r7 (reviewed in Gilland and Baker, 1993). Colocalization of the nVII and nIX nuclei in r7 is not unique to the zebrafish, since it occurs to some degree in the mouse (see above) and extensively in many salamander species (Wake, 1993).

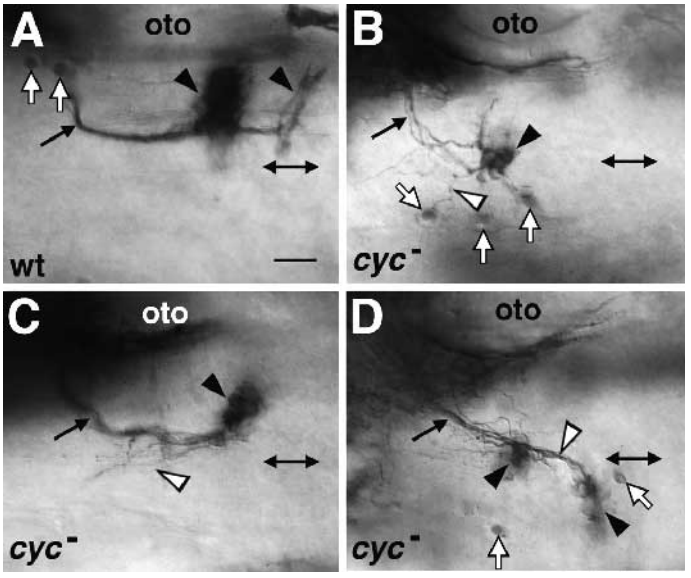

Fig. 9. The *cyc* ^{b16} mutation severely disrupts the specification and axonogenesis of the nVII neurons. All panels show dorsal views with rostral to the left. The nVII neurons and their axons were retrogradely labeled by DiI injection into the hyoid arch on one side in 36 hpf wild-type (A) and *cyc*⁻ (B-D) embryos. Double-headed arrows mark the midline. (A) The nVII neuron clusters (arrowheads) and their axons (black arrow) exhibit the normal characteristics described earlier. (B-D) In mutants, the number of nVII neurons (black arrowheads) is greatly reduced, and they lie on the midline (B,D), or even lie on the contralateral side (D). Some of the axons (black arrows) remain ipsilateral, while others (white arrowheads) cross the midline (B-D). The white arrows in A, B and D indicate stained blood cells, an artifact of photoconversion. oto, otocyst. Bar, 20 μm.

What causes the zebrafish nVII neurons to be located in r6 and r7, rather than in r4 and r5? We propose two hypotheses: (1) nVII neurons are specified in r4, and subsequently migrate caudally into r5, r6 and r7, and (2) the nVII neurons may be specified and remain in r6 and r7 throughout development. Our results and other studies lead us to favor the former hypothesis.

First, analyses of developmental expression of the *tag1* and *isl1* genes indicate that presumptive nVII neurons are located in r4, r5 and r6 early in development (Fig. 6). Since most *isl1*- and *tag1*-expressing cells are located in r6 and r7 a few hours later, these observations are consistent with a caudally directed migration of nVII neurons during development. This interpretation assumes that the *isl1* and *tag1* genes are expressed continuously, and therefore that their expression is a reliable marker for presumptive nVII neurons during the stages at which the cells are monitored. An alternative explanation is that our observations reflect dynamic changes in *isl1* and *tag1* gene expression in different cells located in different rhombomeres.

Second, branchiomotor axon tracing experiments in shark embryos have shown that nVII cell bodies are initially located in r4 and r5, and later appear in r6 (Gilland and Baker, 1992). Furthermore, the characteristic shape of nVII axons, the genu (Fig. 5A), is consistent with neuronal specification in r4 and subsequent caudal migration into their final locations (Gilland and Baker, 1992). Recent experiments suggest that some nVII neurons may also migrate caudally from r4 into r5 and r6 in the mouse (Fritzsch, 1996; Goddard et al., 1996; Studer et al., 1996). Analysis of branchiomotor nuclei in chick/quail chimeras containing rhombomere transplants suggests that nVII neurons can migrate across rhombomere boundaries in the chick as well (Marin and Puelles, 1995). Although a caudally directed migration of nVII neurons is believed to establish the adult pattern of branchiomotor nuclei in many vertebrates (Gilland and Baker, 1993), the zebrafish is unique in that this putative migration of nVII neurons occurs very early during hindbrain development.

Our proposal of inter-rhombomeric neuronal migration may appear to contradict observations from cell-lineage experi-

ments in the chick that the vast majority of cells in adjacent rhombomeres do not mix during early development (Fraser et al., 1990; Birgbauer and Fraser, 1994). It is possible that the few cells that were observed to cross rhombomere boundaries in these studies (Birgbauer and Fraser, 1994) were motor neurons (Marin and Puelles, 1995). Moreover, it is also becoming clear that once the developmental identity of a cell is specified according to its rhombomeric location early in embryogenesis, the cell may move freely across rhombomeres (Lumsden and Krumlauf, 1996). Neuronal migration across rhombomeres may occur by soma translocation within leading processes, which has been implicated in neuronal migration in many vertebrates (Book and Morest, 1990; Gilland and Baker, 1992; Fritzsch et al., 1993). The questions of whether nVII neurons migrate, and their mode of migration, can be addressed by observing vitally labeled, presumptive nVII neurons in vivo with time-lapse microscopy.

Defective motor neuron organization in *valentino* mutant embryos

In mutants of the zebrafish segmentation gene, *valentino*, r5 and r6 fail to be subdivided from a common precursor 'proto-segment'. Consequently, this precursor persists as rX, a region with mixed identity, which fails to form boundaries with either r4 rostrally or r7 caudally. *valentino* is the zebrafish homolog of the mouse *kreisler* gene (Cordes and Barsh, 1994), and encodes a bZIP transcription factor (Moens et al., unpublished). *valentino* is expressed throughout r5 and r6, which is consistent with a cell-autonomous requirement for *val* function in these rhombomeres, as inferred from transplantation experiments (Moens et al., 1996). Also consistent with a cell-autonomous requirement for *val* function in r5 and r6 is the absence in *val*$^-$ embryos of the abducens motor nuclei, which normally differentiate in r5 and r6 (Moens et al., 1996).

We show here that the nVII neurons form disorganized, irregular clumps in *val*$^-$ embryos, and that their axons are poorly fasiculated as they extend toward their exit point in r4. Furthermore, the single cluster of nIX neurons in r7 is absent. Since the numbers of *tag1*-expressing presumptive nVII neurons are comparable in wild-type and *val*$^-$ embryos, the disorganization of the nVII nuclei in mutant embryos may reflect normal specification of nVII neurons in r4 and defective caudal migration due to aberrant r5/6 development. In contrast, the absence of the r7-specific nIX neurons is unexpected in a mutant whose primary and cell-autonomous defect is in r5 and r6, and could result from defects either in signaling or cell migration between rhombomeres. The nIX neurons may normally be induced in r7 by r5/6-derived signals that are absent in *val*$^-$ embryos. Alternatively, the nIX neurons may normally be specified in r5/6 and subsequently migrate caudally into r7. If nIX neurons normally migrate into r7, their absence in r7 of *val*$^-$ embryos may result from their failure to be specified due to aberrant r5/6 development. The characteristic shape of nIX axons in wild-type embryos, the genu (Fig. 3A), is also consistent with neuronal specification in r6 and subsequent caudal migration into r7. In vivo, time-lapse microscopic observations on vitally labeled nIX neurons can address whether these cells migrate caudally during development.

The nVII axons are abnormal in *val*$^-$ embryos (Fig. 7B). Although they are frequently defasciculated, a majority of the axons exhibit normal trajectories, that is, they turn sharply away from the midline in r4 or in the rostral margin of rX. This result suggests that although the motor neurons are disorganized in *val*$^-$ embryos, their axons are able to respond normally to putative guidance cues in r4 or in the rostral margin of rX. Furthermore, since nVII axons are defasciculated in rX in spite of *tag1* gene expression in these neurons (Fig. 7D), it is possible that fasciculation of these axons may involve other cell adhesion molecules whose expression is affected in *val*$^-$ embryos.

The defective branchiomotor phenotype of *val*$^-$ embryos is consistent with the results of gene-disruption experiments in the mouse. In the mouse, the nV neurons are located primarily in r2 and r3, and the nVII neurons are located primarily in r4 and r5. *Krox20*$^-$ mutant embryos, in which r3 and r5 are eliminated, have few nV neurons (Schneider-Maunoury et al., 1993). *Hoxa-1*$^-$ mutant embryos, in which r3 through r8 are affected and r5 is missing, have severely disorganized nVII neurons (Lufkin et al., 1991; Carpenter et al., 1993). *Hoxb-1*$^-$ mutant embryos, in which *Hoxb-1* expression in r4 is eliminated, fail to form the nVII nucleus (Goddard et al., 1996). In mutant embryos, nVII neurons are specified normally in r4, but apparently do not migrate into r5 (Studer et al., 1996), resulting in the absence of the nVII nucleus. Taken together with these results, our analyses demonstrate that rhombomere-specific cues play vital roles in the specification, organization and axonogenesis of the branchiomotor neurons.

Role of ventral midline cells in branchiomotor neuron specification and axon guidance

Our analysis of the branchiomotor phenotype in *cyc*$^-$ embryos suggests that ventral midline cells of the neural tube, probably the floor plate cells, play a major role in the specification of branchiomotor neurons and in preventing their axons from crossing the ventral midline (Fig. 9). Previous studies on axonogenesis by well identified spinal neurons and hindbrain reticulospinal neurons have established the importance of ventral midline structures, including the floor plate cells, in axon guidance in the zebrafish (Bernhardt et al., 1992a,b; Hatta, 1992; Greenspoon et al., 1995). Our observation that the nVII axons frequently cross the ventral midline in *cyc*$^-$ embryos is consistent with a role for floor plate cells in their guidance (Colamarino and Tessier-Lavigne, 1995). Indeed, Guthrie and Pini (1995) have shown that chick branchiomotor axons are repelled by ectopic floor plate cells, suggesting a role for floor plate-derived repulsive cues in normal axonogenesis of these neurons. Alternatively, since the nVII axons may fasciculate with the MLF, as demonstrated for other zebrafish axons (Kuwada et al., 1990; Hatta, 1992), the frequent fusion of the MLF in *cyc*$^-$ embryos (Hatta, 1992) may lead to the midline-crossing phenotype of nVII axons in mutant embryos. Misexpression studies with genes encoding growth-cone repelling molecules, which are specifically expressed in the floorplate cells (Halloran et al., 1996), will allow for an assessment of the role of growth cone repulsion in branchiomotor axon guidance.

We thank Mary Halloran, Bill Jackman, Jim Lauderdale, Wataru Shoji and Kathryn Tosney for comments on the manuscript, Ed Gilland and Bernd Fritzsch for discussion, Su Fengyun and Kana Takahashi for fish care, and David Bay for invaluable photographic assistance. We thank Bill Trevarrow for the zn5 antibody, Grace Pan-

ganiban for the distal-less antibody and Bruce Appel for the *isl1* gene probe. The 39.4D5 islet antibody developed by T. Jessell was obtained from the Developmental Studies Hybridoma Bank maintained by the Department of Biological Sciences, University of Iowa, under contract NO1-HD-7-3263 from the NICHD. This work was supported by post-doctoral fellowships from the Center for Organogenesis, University of Michigan (A.C.), the Human Frontier Science Program (C.B.M.) and the Paralysed Veterans of America/Spinal Cord Research Foundation (J.T.W.), and by grants from the Muscular Dystrophy Association (J.Y.K.), NINDS NS24848 (J.Y.K.) and NS17963 (C.B.K.).

REFERENCES

Akimenko, M. A., Ekker, M., Wegner, J., Lin, W. and Westerfield, M. (1994). Combinatorial expression of three zebrafish genes related to *distal-less*: part of a homeobox gene code for the head. *J. Neurosci.* **14,** 3475-3486.

Appel, B., Korzh, V., Glasgow, E., Thor, S., Edlund, T., Dawid, I. B. and Eisen, J. S. (1995). Motoneuron fate specification revealed by patterned LIM homeobox gene expression in embryonic zebrafish. *Development* **121,** 4117-4125.

Bernhardt, R. R., Nguyen, N. and Kuwada, J. Y. (1992a). Growth cone guidance by floor plate cells in the spinal cord of zebrafish embryos. *Neuron* **8,** 869-882.

Bernhardt, R. R., Patel, C. K., Wilson, S. W. and Kuwada, J. Y. (1992b). Axonal trajectories and distribution of GABAergic spinal neurons in wildtype and mutant zebrafish lacking floor plate cells. *J. Comp. Neurol.* **326,** 263-272.

Birgbauer, E. and Fraser, S. E. (1994). Violation of cell lineage restriction compartments in the chick hindbrain. *Development* **120,** 1347-1356.

Book, K. J. and Morest, D. K. (1990). Migration of neuroblasts by perikaryal translocation: Role of cellular elongation and axonal outgrowth in the acoustic nuclei of the chick embryo medulla. *J. Comp. Neurol.* **297,** 55-76.

Burrill, J. D. and Easter, S. S., Jr. (1994). Development of the retinofugal projections in the embryonic and larval zebrafish (*Brachydanio rerio*). *J. Comp. Neurol.* **346,** 583-600.

Carpenter, E. M., Goddard, J. M., Chisaka, O., Manley, N. R. and Capecchi, M. R. (1993). Loss of *Hox-a1* (*Hox-1.6*) function results in the reorganization of the murine hindbrain. *Development* **118,** 1063-1075.

Chisaka, O., Musci, T. S. and Capecchi, M. R. (1992). Developmental defects of the ear, cranial nerves and hindbrain resulting from targeted disruption of the mouse homeobox gene *Hox-1.6*. *Nature* **355,** 516-520.

Chitnis, A. B. and Kuwada, J. Y. (1990). Axonogenesis in the brain of zebrafish embryos. *J. Neurosci.* **10,** 1892-1905.

Colamarino, S. A. and Tessier-Lavigne, M. (1995). The role of the floor plate in axon guidance. *Annu. Rev. Neurosci.* **18,** 497-529.

Cordes, S. P. and Barsh, G. S. (1994). The mouse segmentation gene *kr* encodes a novel basic domain-leucine zipper transcription factor. *Cell* **79,** 1025-1034.

Driever, W., Stemple, D., Schier, A. and Solnica-Krezel, L. (1994). Zebrafish: genetic tools for studying vertebrate development. *Trends Genet.* **10,** 152-159.

Fashena, D. S. (1996). A neuron's reach can exceed its GRASP: expression of a cell adhesion molecule in the zebrafish embryo. Ph.D. Thesis, University of Oregon.

Fraser, S., Keynes, R. and Lumsden, A. (1990). Segmentation in the chick embryo hindbrain is defined by cell lineage restrictions. *Nature* **344,** 431-435.

Fritzsch, B., Christensen, M. A. and Nichols, D. H. (1993). Fiber pathways and positional changes in efferent perikarya of 2.5- to 7-day chick embryos as revealed with DiI and dextran amines. *J. Neurobiol.* **24,** 1481-1499.

Fritzsch, B. (1996). Development of the labyrinthine efferent system. *Ann. N.Y. Acad. Sci.* **781,** 21-33.

Frohman, M. A., Martin, G. R., Cordes, S. P., Halamek, L. P. and Barsh, G. S. (1993). Altered rhombomere-specific gene expression and hyoid bone differentiation in the mouse segmentation mutant, *kreisler* (*kr*). *Development* **117,** 925-936.

Furley, A. J., Morton, S. B., Manalo, D., Karagogeos, D., Dodd, J. and Jessell, T. M. (1990). The axonal glycoprotein TAG-1 is an immunoglobulin superfamily member with neurite outgrowth-promoting activity. *Cell* **61,** 157-170.

Gilland, E. and Baker, R. (1992). Longitudinal and tangential migration of cranial nerve efferent neurons in the developing hindbrain of *Squalus acanthias*. *Biol. Bull.* **183,** 356-358.

Gilland, E. and Baker, R. (1993). Conservation of neuroepithelial and mesodermal segments in the embryonic vertebrate head. *Acta Anat.* **148,** 110-123.

Goddard, J. M., Rossel, M., Manley, N. R. and Capecchi, M. R. (1996). Mice with targeted disruption of *Hoxb-1* fail to form the motor nucleus of the VIIth nerve. *Development* **122,** 3217-3228.

Goodman, C. S. and Shatz, C. J. (1993). Developmental mechanisms that generate precise patterns of neuronal connectivity. *Neuron* **10 (Suppl.),** 77-98.

Greenspoon, S., Patel, C. K., Hashmi, S., Bernhardt, R. R. and Kuwada, J. Y. (1995). The notochord and floor plate guide growth cones in the zebrafish spinal cord. *J. Neurosci.* **15,** 5956-5965.

Guthrie, S. and Pini, A. (1995). Chemorepulsion of developing motor axons by the floor plate. *Neuron* **14,** 1117-1130.

Halloran, M. C., Yee, C. S., Severance, S. and Kuwada, J. Y. (1996). Cloning and analysis of three zebrafish semaphorins. *Soc. Neurosci. Abstr.* **22, Part 2,** 1472.

Hatta, K., Schilling, T. F., BreMiller, R. A. and Kimmel, C. B. (1990). Specification of jaw muscle identity in zebrafish: correlation with engrailed-homeoprotein expression. *Science* **250,** 802-805.

Hatta, K., Kimmel, C. B., Ho, R. K. and Walker, C. (1991). The *cyclops* mutation blocks specification of the floor plate of the zebrafish central nervous system. *Nature* **350,** 339-341.

Hatta, K. (1992). Role of the floor plate in axonal patterning in the zebrafish CNS. *Neuron* **9,** 629-642.

Inoue, A., Takahashi, M., Hatta, K., Hotta, Y. and Okamoto, H. (1994). Developmental regulation of *islet-1* mRNA expression during neuronal differentiation in embryonic zebrafish. *Dev. Dyn.* **199,** 1-11.

Kanki, J. P., Chang, S. and Kuwada, J. Y. (1994). The molecular cloning and characterization of potential chick DM-GRASP homologs in zebrafish and mouse. *J. Neurobiol.* **25,** 831-845.

Kimmel, C. B., Metcalfe, W. K. and Schabtach, E. (1985). T reticular interneurons: a class of serially repeating cells in the zebrafish hindbrain. *J. Comp. Neurol.* **233,** 365-376.

Kimmel, C. B. (1993). Patterning the brain of the zebrafish embryo. *Annu. Rev. Neurosci.* **16,** 707-732.

Kimmel, C. B., Ballard, W. W., Kimmel, S. R., Ullmann, B. and Schilling, T. F. (1995). Stages of embryonic development of the zebrafish. *Dev. Dyn.* **203,** 253-310.

Korzh, V., Edlund, T. and Thor, S. (1993). Zebrafish primary neurons initiate expression of the LIM homeodomain protein Isl-1 at the end of gastrulation. *Development* **118,** 417-425.

Kuwada, J. Y., Bernhardt, R. R. and Chitnis, A. B. (1990). Pathfinding by identified growth cones in the spinal cord of zebrafish embryos. *J. Neurosci.* **10,** 1299-1308.

Kuwada, J. Y. (1995). Development of the zebrafish nervous system: genetic analysis and manipulation. *Curr. Opin. Neurobiol.* **5,** 50-54.

Lubke, J. (1993). Photoconversion of diaminobenzidine with different fluorescent neuronal markers into a light and electron microscopic dense reaction product. *Micro. Res. Tech.* **24,** 2-14.

Lufkin, T., Dierich, A., LeMeur, M., Mark, M. and Chambon, P. (1991). Disruption of the *Hox-1.6* homeobox gene results in defects in a region corresponding to its rostral domain of expression. *Cell* **66,** 1105-1119.

Lumsden, A. and Keynes, R. (1989). Segmental patterns of neuronal development in the chick hindbrain. *Nature* **337,** 424-428.

Lumsden, A. and Krumlauf, R. (1996). Patterning the vertebrate neuraxis. *Science* **274,** 1109-1115.

Lumsden, A., Sprawson, N. and Graham, A. (1991). Segmental origin and migration of neural crest cells in the hindbrain region of the chick embryo. *Development* **113,** 1281-1291.

Marin, F. and Puelles, L. (1995). Morphological fate of rhombomeres in quail/chick chimeras: A segmental analysis of hindbrain nuclei. *Eur. Jour. Neurosci.* **7,** 1714-1738.

Marshall, H., Nonchev, S., Sham, M. H., Muchamore, I., Lumsden, A. and Krumlauf, R. (1992). Retinoic acid alters hindbrain Hox code and induces transformation of rhombomeres 2/3 into a 4/5 identity. *Nature* **360,** 737-741.

McConnell, S. K. (1995). Strategies for the generation of neuronal diversity in the developing central nervous system. *J. Neurosci.* **15,** 6987-6998.

McKay, I. J., Muchamore, I., Krumlauf, R., Maden, M., Lumsden, A. and Lewis, J. (1994). The *kreisler* mouse: a hindbrain segmentation mutant that lacks two rhombomeres. *Development* **120,** 2199-2211.

Moens, C. B., Yan, Y.-L., Appel, B., Force, A. and Kimmel, C. B. (1996).

valentino: a zebrafish gene required for normal hindbrain segmentation. *Development* **122**, 3981-3990.

Moody, S. A. and Heaton, M. B. (1983). Developmental relationships between trigeminal ganglia and trigeminal motoneurons in chick embryos. II. Ganglion axon ingrowth guides motoneuron migration. *J. Comp. Neurol.* **213,** 344-349.

Noden, D. M. (1983). The role of the neural crest in patterning of avian cranial skeletal, connective and muscle tissues. *Dev. Biol.* **96,** 144-165.

Nusslein-Volhard, C. (1994). Of flies and fishes. *Science* **266,** 572-574.

Panganiban, G., Sebring, A., Nagy, L. and Carroll, S. (1995). The development of crustacean limbs and the evolution of arthropods. *Science* **270,** 1363-1367.

Pfaff, S. L., Mendelsohn, M., Stewart, C. L., Edlund, T. and Jessell, T. M. (1996). Requirement for LIM homeobox gene *Isl1* in motor neuron generation reveals a motor neuron-dependent step in interneuron differentiation. *Cell* **84,** 309-320.

Piperno, G. and Fuller, M. T. (1985). Monoclonal antibodies specific for an acetylated form of alpha-tubulin recognize the antigen in cilia and flagella from a variety of organisms. *J. Cell Biol.* **101,** 2085-2094.

Schilling, T. F. and Kimmel, C. B. (1994). Segment and cell type lineage restrictions during pharyngeal arch development in the zebrafish embryo. *Development* **120,** 483-494.

Schneider-Maunoury, S., Topilko, P., Seitandou, T., Levi, G., Cohen-Tannoudji, M., Pournin, S., Babinet, C. and Charnay, P. (1993). Disruption of *Krox-20* results in alteration of rhombomeres 3 and 5 in the developing hindbrain. *Cell* **75,** 1199-1214.

Stoeckli, E. T. and Landmesser, L. T. (1995). Axonin-1, Nr-CAM, and Ng-CAM play different roles in the in vivo guidance of chick commissural neurons. *Neuron* **14,** 1165-1179.

Studer, M., Lumsden, A., Ariza-McNaughton, L., Bradley, A. and Krumlauf, R. (1996). Altered segmental identity and abnormal migration of motor neurons in mice lacking *Hoxb-1*. *Nature* **384,** 630-634.

Swiatek, P. J. and Gridley, T. (1993). Perinatal lethality and defects in hindbrain development in mice homozygous for a targeted mutation of the zinc finger gene *Krox20*. *Genes Dev.* **7,** 2071-2084.

Tanabe, Y. and Jessell, T. M. (1996). Diversity and pattern in the developing spinal cord. *Science* **274,** 1115-1123.

Trevarrow, B., Marks, D. L. and Kimmel, C. B. (1990). Organization of hindbrain segments in the zebrafish embryo. *Neuron* **4,** 669-679.

Wake, D. B. (1993). Brainstem organization and branchiomeric nerves. *Acta Anat.* **148,** 124-131.

Warren, J. T., Jr., Kanki, J. P., Rangarajan, R., Furley, A. and Kuwada, J. Y. (1995). Molecular cloning and expression analysis of zebrafish TAG-1. *Soc. Neurosci. Abstr.* **21, Part 1,** 533.

Westerfield, M. (1995). *The Zebrafish Book*. University of Oregon; Eugene, OR.

(Accepted 17 April 1997)